IIETA International Information and Engineering Technology Association
Advancing the World of Information and Engineering

Traitement du Signal
Vol. 42, No. 1, February, 2025, pp. 87-99
Journal homepage: http://iieta.org/journals/ts

CNN Architecture Based Classification of Hemorrhagic and Ischemic Stroke Using MR Images

Srisabarimani Kaliannan, Arthi Rengaraj*

Department of ECE, SRM Institute of Science and Technology, Ramapuram, Chennai 600089, India

Corresponding Author Email: arthir2@srmist.edu.in

https://doi.org/10.18280/ts.420109

Received: 21 September 2023
Revised: 6 April 2024
Accepted: 25 September 2024
Available online: 28 February 2025

Keywords:
ischemic, hemorrhagic, Gradient Echo Image (GRE), Diffusion-Weighted Imaging (DWI), Susceptibility Weighted Image (SWI), CNN

ABSTRACT

Hemorrhagic and ischemic strokes are major medical conditions that require timely intervention and diagnosis to reduce brain injury and enhance patient outcomes. In recent years, magnetic resonance imaging (MRI) methods like Diffusion-Weighted Imaging (DWI), Gradient Echo Image (GRE), and Susceptibility Weighted Image (SWI), have become increasingly important in the diagnosis and management of these conditions. The suggested system's innovation is to use CNN architecture with binary classification to classify hemorrhagic and ischemic brain strokes using various imaging techniques for early diagnosis and treatment with the highest accuracy. A real-time dataset of 40 Hemorrhagic, and 34 Ischemic MRI scans has been used to find the accuracy for classifying the brain damage. The simulated results show that all four models of CNN Architecture achieve good accuracy in classifying hemorrhagic and ischemic strokes based on advanced MR Image sequences like DWI, GRE, and SWI. Our results demonstrated the highest accuracy rate for DenseNet and GoogleNet achieving 97.30% while AlexNet and ResNet obtained an accuracy rate of 95.95% and 94.59% respectively.

1. INTRODUCTION

Ischaemic and hemorrhagic strokes are two distinct forms of strokes that affect the brain and can have serious consequences. While both conditions involve the interruption of the flow of blood to the brain, they have different underlying factors and require different approaches to treatment. Ischemic stroke is the predominant form, comprising over 87% of all stroke cases. A stroke occurs when there is a blockage or narrowing of an artery supplying blood to the brain. A blood clot (thrombus) that forms within the arterial vessel (thrombotic stroke) or a clot or other debris that travels from another region of the body and lodges in a brain artery (embolic stroke) can both be the source of this blockage. Brain cells are oxygen and nutrition deficient as a result of the reduced blood flow, resulting in their damage or death. Ischemic strokes are often associated with common risk factor including high blood pressure, smoking, diabetes, high cholesterol, sedentary lifestyle.

In contrast, A hemorrhagic stroke occurs when a blood vessel in the brain ruptures, leading to bleeding within or around the brain tissue. Arteriovenous malformations (abnormal connections between arteries and veins), head trauma, aneurysms (weakened portions in blood vessel walls), and hypertension are some of the confusions that might origin this bleeding. The rupture results in the accumulation of blood, which can potentially damage brain cells and increase the pressure on the brain. Hemorrhagic strokes are less prevalent than ischaemic strokes; however, they are associated with higher mortality rates.

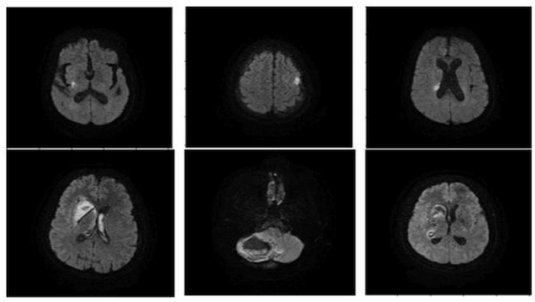

Figure 1. Samples of stroke types in DWI, SWI MR images

Figure 1 shows the samples of stroke types in DWI, and SWI MR Images. abrupt weakness or numbness on one side of the body, complexity in speaking or accepting speech, severe headache, vertigo, and decline in incoordination or stability are among the symptoms that both types of strokes share. Regardless of the situation, it is essential to promptly recognize and seek medical attention, as immediate treatment can reduce brain injury and increase the likelihood of recovery. Ischaemic and hemorrhagic strokes necessitate distinct treatment strategies. The treatment of ischaemic stroke frequently entails the administration of thrombolytics, which dissolve clots, to restore blood flow, or procedures like mechanical clot retrieval, which physically removes the clot. Hemorrhagic stroke treatment, in contrast, emphasizes the prevention of additional complications, the alleviation of cerebral pressure, and the regulation of bleeding. This may necessitate operative interventions, blood pressure

medication, and other supportive measures. Ischemic stroke stems from the blockage of blood circulation to the brain, while hemorrhagic stroke occurs as a result of the rupture of the blood vein. Recognizing the signs and obtaining quick medical assistance is critical for both illnesses to reduce brain damage and improve outcomes.

The novelty of the proposed system is it uses CNN Architecture, which uses binary classification to classify hemorrhagic and ischemic strokes using various imaging techniques like DWI, SWI, and GRE MR Images are taken into consideration for the early diagnosis to treat with the highest accuracy.

Table 1 describes the CNN architecture with various Net for the number of layers, types of layers, and hyper parameters incorporated into the suggested system.

Table 1. Tabulation of various parameters for CNN

CNN Architecture	No. of Layers	Types of Layers	Hyper Parameters
ResNet101	101	ResNet-101 has 101 layers, including convolutional, pooling, fully connected, and batch normalization layers	Max pooling
Densenet169	169	Input Layer, Initial Convolutional Layer, Dense Blocks (x4), Transition Layers, Global Average Pooling (GAP) Layer, Fully Connected Layer, SoftMax Output Layer	Max pooling
GoogleNet	22	Input Layer, Inception Modules (x9), Intermediate Max-Pooling Layers, Auxiliary Classifiers, Global Average Pooling (GAP) Layer, Fully Connected Layer, batch normalization layers	Max pooling
AlexNet	5 Conv 3 FC	Convolutional Layer, Fully Connected Layer	Max pooling

2. LITERATURE REVIEW

Ischemic and hemorrhagic stroke classification utilizing brain MR imaging sequences is one of the most hotly debated research subjects in the scientific world today. To identify brain strokes, Electroencephalography, and augmented reality were incorporated into the brain-computer interface model. The earliest identified properties from EEG signals by the proposed method are spatial and spectral. Regularized discriminant analysis is used to extract and categorize the detected features. To improve classification performance, a kernel density estimation function is added, which offers more trustworthy finding results than conventional methods [1]. To determine which machine learning model performs the best at detecting strokes, a comparison of several models is presented. The experiment used techniques for data selection and examined how well machine learning models performed in the presence and absence of data resampling and imputation. This paper determines from their observations that the random forest method has superior performance compared to other algorithms at predicting strokes [2]. A reliable model for segmenting stroke lesions is described, with the initial step estimating the segmentation using a Bayesian approach. Gabor texture characteristics are employed to further refine the segmentation of the stroke lesion, making it possible to automatically determine the ground truth for strokes with an improved accuracy and dice coefficient than with existing finding methods [3]. The detection of ischemic stroke using medical data is discussed in an examination and comparison of machine learning techniques. The modified random forest model overcomes the constraints in figuring out risk variables in strokes, and the results are evaluated in comparison to conventional methods. During the experimental phase of research, the random forest approach outperformed additional prediction models that are based on machine learning in terms of prediction accuracy [4]. Stroke detection and classification using an adaptive clustering distorted birth iterative approach is given and contrasted with other contrast source inversion-based detection algorithms. The method that is being discussed groups the electrical characteristics of the brain imaging data that was collected using a head scanner. The clustering-based detection model has been found to have improved reconstruction and minimized error [5]. The brain stroke detection model incorporates a hybrid fuzzy model, which outperforms conventional machine learning methods in terms of detection accuracy. Several hybrid and image enhancement techniques have been developed to boost the accuracy of picture categorization in image processing applications. Rough sets and fuzzy sets are used to modify the fuzzy c-means method to enhance the efficacy of segmentation. At first, the statistical attributes are extracted using a grey-level co-occurrence matrix. The method that is being given uses GLCM for feature extraction and fuzzy c means for picture fragmentation. The features are finally categorized utilizing support vector machine, which yields increased precision with less computational effort [6]. A model for segmenting stroke lesions based on deep learning and the multi-input UNet method is given. The method described here extracts features from MR images, including details on the brain's parcellation, the lateral ventricle, white matter, and grey matter. To upgrade segmentation precision, the inputs are fed into a two-channel UNet and concatenated. In comparison to conventional techniques, the presented UNet model achieved improved segmentation, precision, and dice score [7]. The automatic segmenting of brain computed tomographic images for hemorrhage strokes using stroke detection is to use U-Net model built on a specific architecture. Define the symmetry constraints, network that is being presented combines the original picture slice cut with the switched image. Additionally, a process known as adversarial training is added to improve segmentation accuracy. Current U Net achieved an improved dice score, accuracy, and reliability as clinical decision assistance systems when compared to previous techniques [8]. The limitations of conventional techniques are addressed by a machine learning applied in stroke prediction model. The provided method minimizes both high-test cost, lengthy processing time. Convolutional neural networks and long-term memory, short term memory techniques were used during the ensemble model that was displayed to create an ensemble classifier. In comparison to conventional random forest, decision tree algorithms, experimental data showed that ensemble models performed better [9]. Convolutional neural

network is incorporated into stroke detection model that is based on deep learning has been reported to identify ischemic and hemorrhagic strokes. CNN technique is utilised for the purpose of extracting and categorize characteristics in the brain computed tomography pictures it is then compared against Support Vector Machines (SVM), K-Nearest Neighbor (KNN), Random Forests (RF), decision trees, multi-layer perceptron-based detection. Suggested convolution Neural Network based model performed better than alternatives based on machine learning offers more stroke reliability [10, 11]. The model for detecting ischaemic strokes described is a mixed model uses support vector machine to classify features after extracting them initially using high order bi-spectrum entropy. According to the features, the provided technique divides stroke types into three severity categories: high, medium, and mild. Human treatments are avoided because of their excellent specificity and accuracy levels, which eases the burden of routine screening on neurologists [12]. A monitoring system is used to analyse the intricate electric permittivity of the brain's tissues for the early diagnosis of brain strokes. Synthetic results for the detection model are generated using an experimental microwave tomography-based device. The potential for influencing hemorrhage strokes is recognized by highly parallel computation and the application of regularization and domain decomposition techniques [13]. A model for automatic stroke diagnosis is proposed that uses characteristics extracted using discrete curvelet transformation to identify irregularities. To determine the importance of detection, the features are retrieved at various scales. Support vector machines are used to classify the extracted multidirectional statistical information with greater accuracy than previous techniques [14]. The detection of ischemic stroke is discussed using process control model in multivariate statistics. Generally, Heart rate variability is influenced by ischemic stroke has an impact on nervous system activities. To identify ischemic strokes, these variations are used and examined. Rat experiments conducted in real time have shown that the proposed technique achieves average specificity and sensitivity [15]. Brain pictures acquired using magnetic induction tomography are analysed utilising the given hemorrhagic stroke detection model. The pictures acquired using induction tomography are examined and stroke is detected with the least amount of reconstruction and applying the split Bregman algorithm with adaptive thresholding based on weighted frequency difference. Based on experimental observations, the proposed technology exhibits a lower reconstruction error [16]. A fractional approach Darwinian particle swarm method of optimization technique and Delaunay triangulation are used to identify three different stroke varieties identified through magnetic resonance imaging (MRI) data. The proposed optimized model may detect whole an anterior circulation stroke refers to the stroke that affects the front section of the cerebrum's blood supply. Lacunar syndrome is a state characterised by little, deep strokes in the cerebrum. Partial anterior circulation syndrome refers to a stroke that affects only a portion of the front part of the brain's blood supply. By utilizing Support Vector Machines (SVM), Decision Trees (DT), and random forests, the proposed approach categorizes the morphological and statistical aspects. Results showed that decision trees outperform other models at identifying various stroke types [17]. This research presents an approach for Brain lesions generated using a deep generative adversarial network diagnosis using MR pictures [18]. In the recommended approach, convex optimization and deep learning methods applied. In specifically, A globally optimised multi-region time-implicit contour evolution technique, utilising convex relaxation, combines learnt semantic information from convolutional neural networks with local visual context and a high-level user-initialized prior [19]. This work predicts HT's location in AIS using perfusion-weighted magnetic resonance imaging (PWI) and Diffusion-Weighted Imaging (DWI). This study involved retrospective analysis of group of patients with acute ischemic stroke (AIS) who are undergoing reperfusion therapy treatment in one stroke facility [20]. This article Outlines the empirical validation of a microwave imaging system used as monitoring post acute cerebrum stroke in real time. Framework employs sensor device with simple and multi frequency microwave visualisation approach that has unique feature to reduce artefacts [21]. Classification of cerebral stroke using DWI brain images and A model that combines the 3D EmbedConvNext and 3D Bi-LSTM networks [22]. To provide medical care for individuals suffering from cerebral infarctions, this study recommends branded new computerized segmentation and classification systems able to find hemorrhage and ischemia lesions (infarcts) from non-contrast computed tomography scan images. The primary purpose regarding U-Net segmentation is to computerize the identification of stroke type injury having a high level of level of precision [23]. Author presented a fusion-based approach as detecting cerebrum tumours in MR images. Employing a Machine Learning algorithm [24]. This work proposes A comprehensive pattern recognition system that combines clinical signs and quantitative electroencephalogram features system that takes use of electroencephalogram (EEG) data's quick and sensitive reaction, it integrates cerebral ischaemia with clinical indications. By adding leftover units and cascade of ideas principles to the 3DCNN network incorporates cascaded 3D deep residual network for stroke detection accurate method of dividing or partitioning into segments is created. These segmentation algorithms's training set assessment metrics are DICE coefficient, precision, sensitivity. Experimental finding shows that the suggested strategy performs better than current clinical diagnosis strategies. By incorporating this restriction utilising the data gathered from various sources, A lightweight convolution model consisting of two step is developed. The provided CT scans are the input delivered to the architecture used is VGG-16 the first stage, and the data frameworks are provided to random forest in the second step for the segmentation of strokes into three classes [24].

3. PROPOSED METHOD

The existing method normally detects the occurrence of stroke cases through magnetic resonance imaging (MRI) and does not provide a clear classification of stroke varieties. The proposed system's novelty is it has used CNN Architecture to classify the hemorrhagic and ischemic strokes using various imaging techniques for early detection and most accurate treatment. Figure 2 illustrates the proposed architecture to classify the stroke classification using MR image to determine the accuracy, multiple CNN architectures are employed. Figure 3 shows the flow process to classify the stroke types utilizing Magnetic Resonance Image to determine accuracy with the use of various CNN architectures.

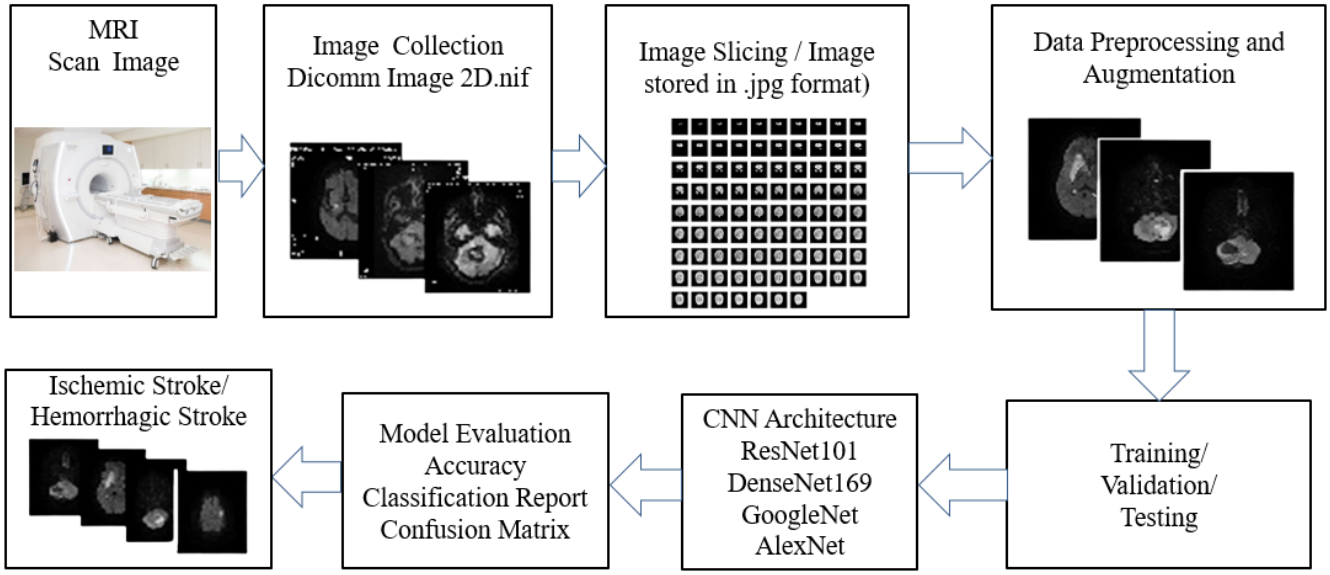

Figure 2. Proposed architecture for categorisation of hemorrhagic and ischemic brain stroke types using MRI

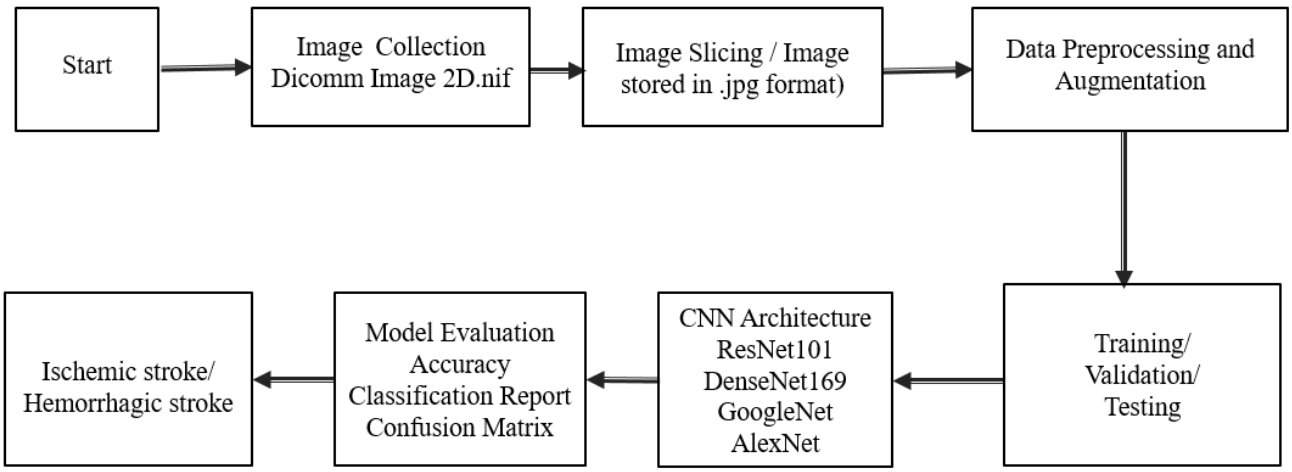

Figure 3. Flow process for categorisation of hemorrhagic and ischemic brain stroke types using MRI

1. Data Collection: In this phase, dataset of DICOMM MR Images stored in neuroimaging informatics initiative file format for hemorrhagic and ischemic stroke patients was collected that includes DWI, GRE, and SWI MRI data. The collected images are sliced for data preprocessing.

2. Data Preprocessing: The collected real time dataset was preprocessed to remove any noise or artifacts present in the images. The images were also normalized and resized to a standard size to ensure consistency across the dataset. The real-time dataset was augmented using the function Fastai to increase the number of images for training the CNN models. The dataset is splinted randomly for training with 20% of validation.

3. Model Selection: Four popular CNN architectures namely ResNet, DenseNet, GoogleNet, and AlexNet were selected to classify the type of stroke to get an early evaluation and the best possible treatment.

4. Model Training: The selected models were trained with 20% of validation on the preprocessed dataset making use of transfer learning. It is widely utilised approach in deep learning where a pre-trained model is utilised and adjusted to perform a given goal. In this case, the models were refined after being pre-trained on a big dataset of generic photos on the MRI dataset for hemorrhagic and ischemic brain stroke classification.

5. Model Evaluation: After training, the accuracy of the models was assessed by evaluating them on a test dataset. The evaluation metrics utilised are accuracy, precision, recall, F1 score, confusion matrix, and categorisation report. SGD optimizer was chosen with binary cross entropy loss for model compilation. A batch size of eight is selected and a model learning rate of 0.001.

4. RESULTS AND DISCUSSION

To determine the occurrence of hemorrhagic and ischemic brain stroke, performance criteria such as classification report, precision, recall, F1 score, accuracy, and confusion matrix were found for CNN Architecture like ResNet, DenseNet, GoogleNet, and AlexNet.

4.1 ResNet 101

The Residual Network supports thousands of convolutional layers to overcome vanishing gradient problem. Figure 4 shows the functional block diagram of ResNet that explains to classify the stroke such as hemorrhagic or Ischemic.

In order to train the model with lower learning rates, the parameters are unfrozen and the model has been trained to obtain minimum, steep, valley and slide levels as shown in Figure 5 Out of these, the steepest level has been fine-tuned with the baseline model by the learning rate finder for the ResNet101.

Figure 6 displays training loss and validation loss, error rate for Resnet101. As epoch increases, the loss decreases for both training loss and validation loss and error rate becomes constant after particular epochs.

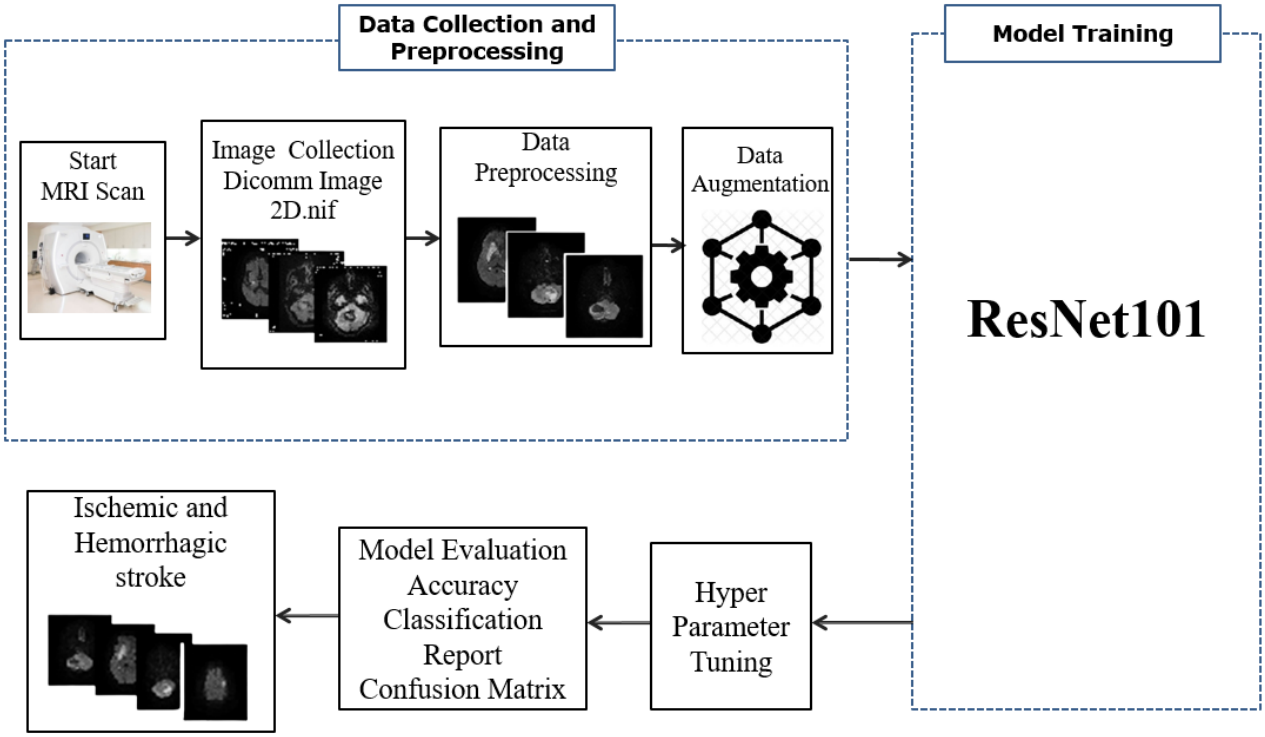

Figure 4. Functional block diagram - ResNet101

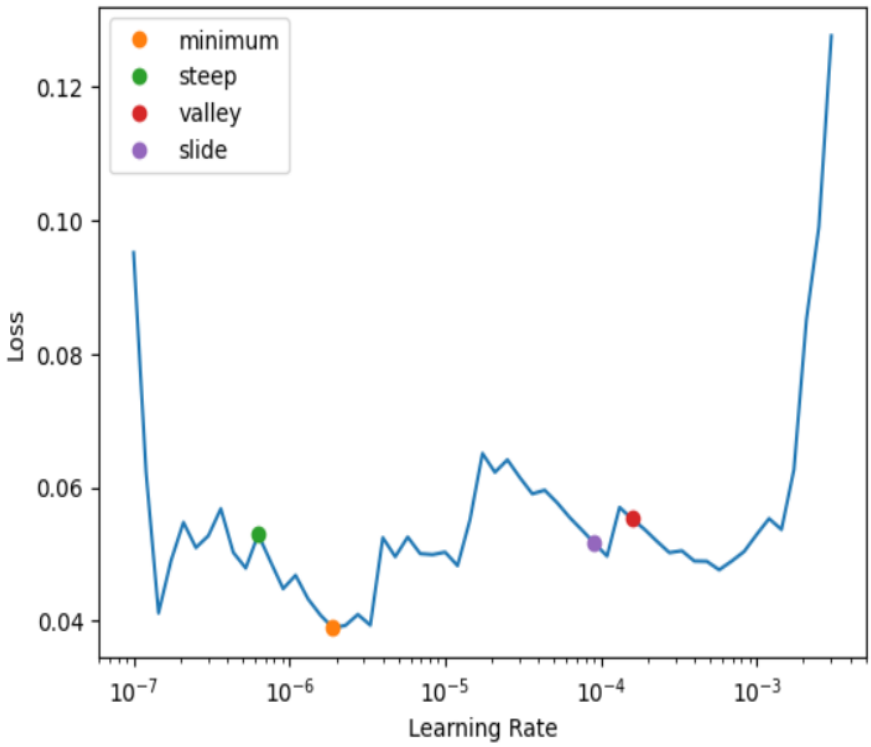

Figure 5. Learning rate finder for ResNet101

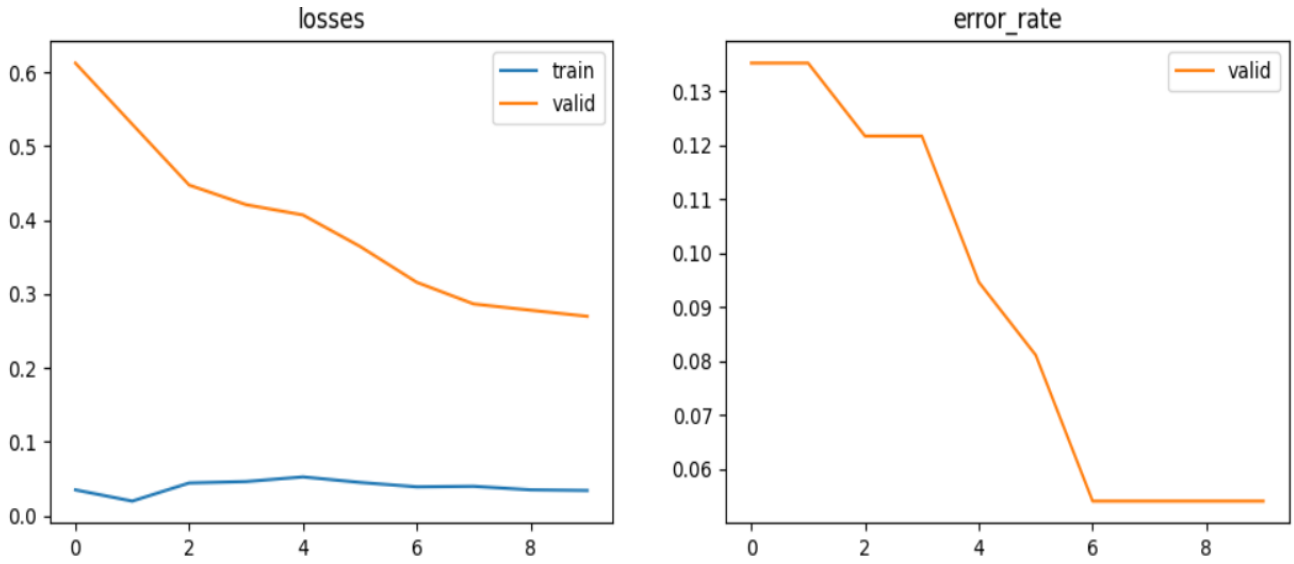

Figure 6. Graphical representation of training and validation loss, error rate- ResNet101

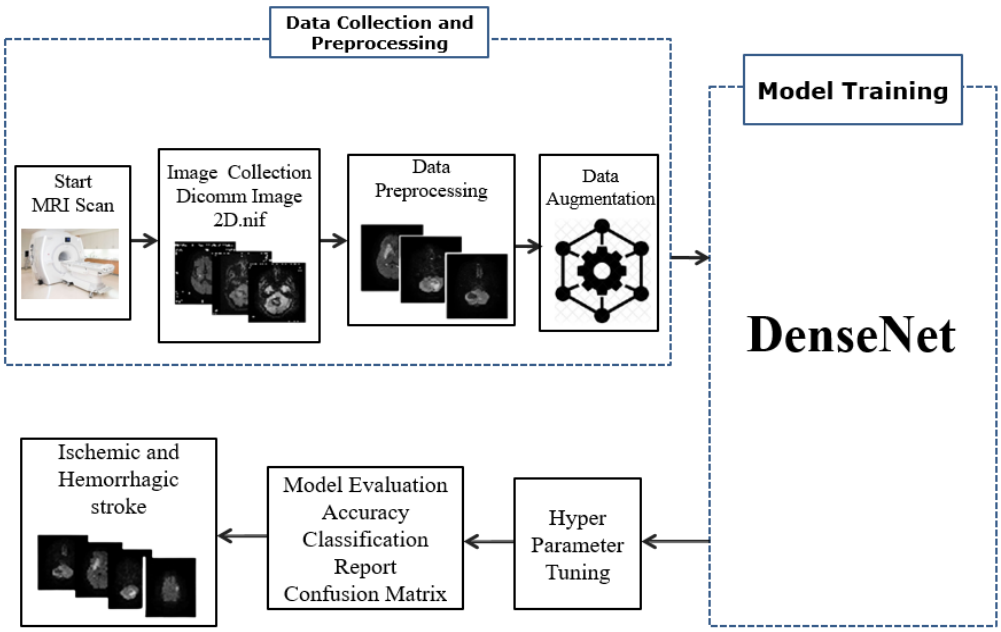

Figure 7. Functional block diagram of DenseNet169

Table 2 illustrates duration required for each epoch in terms of training, validation loss, and error rate.

Table 2. Table for epochs over training, validation loss and error rate - ResNet101

Epoch	Train_Loss	Val_Loss	Err_Rate	T (ms)
0	0.034895	0.612339	0.135135	00:09
1	0.019673	0.529657	0.135135	00:06
2	0.044201	0.447303	0.121622	00:06
3	0.046116	0.420772	0.121622	00:06
4	0.052440	0.406878	0.094595	00:07
5	0.044965	0.364443	0.081081	00:06
6	0.038987	0.315771	0.054054	00:06
7	0.039701	0.286445	0.054054	00:06
8	0.034920	0.277958	0.054054	00:07
9	0.034056	0.269686	0.054054	00:07

4.2 DenseNet169

DenseNet169 takes all previous output as an input for a future layer. Figure 7 displays functional block diagram of DenseNet169 that explains to classify the stroke such as hemorrhagic or Ischemic.

The parameters are unfrozen to obtain the learning rate as shown in Figure 8 Out of these, the slide and minimum level attained the finetuning with baseline model by the learning rate finder for the DenseNet169.

Figure 9 illustrates the training loss and validation loss for unfreeze DenseNet169. Training loss and validation vary accordingly based on the performance of DenseNet169 Training for unfreeze layers.

Figure 10 displays training and validation loss and error rate for DenseNet169. As the unit of epoch rises, the loss decreases for both training and validation and the error rate becomes constant after particular epochs.

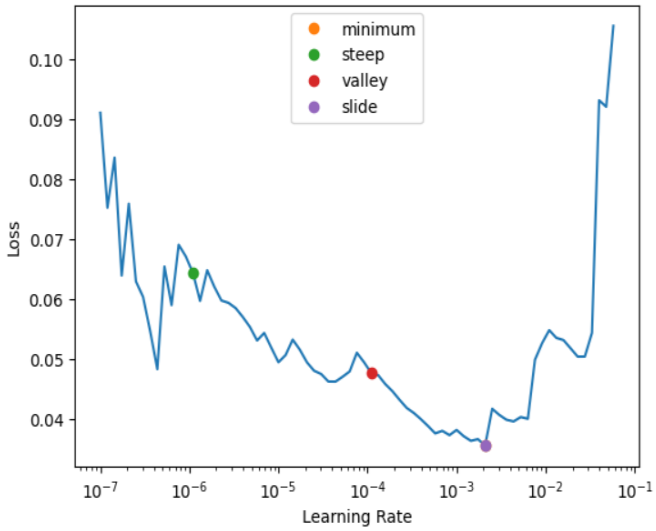

Figure 8. Learning rate finder for DenseNet169

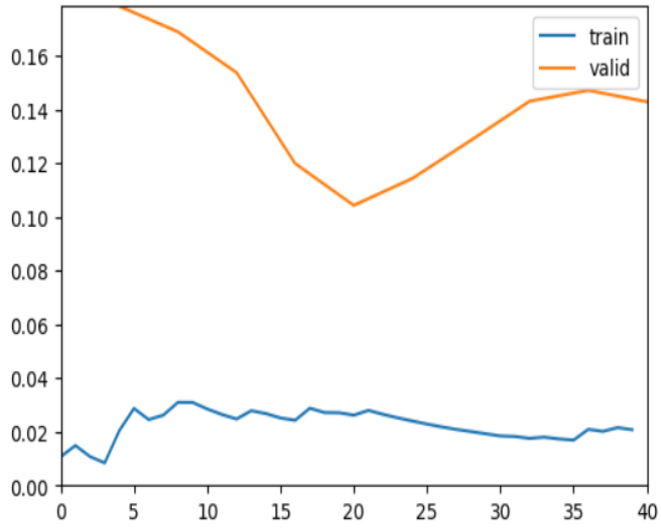

Figure 9. Graphical representation of training, validation loss for unfreeze DenseNet169

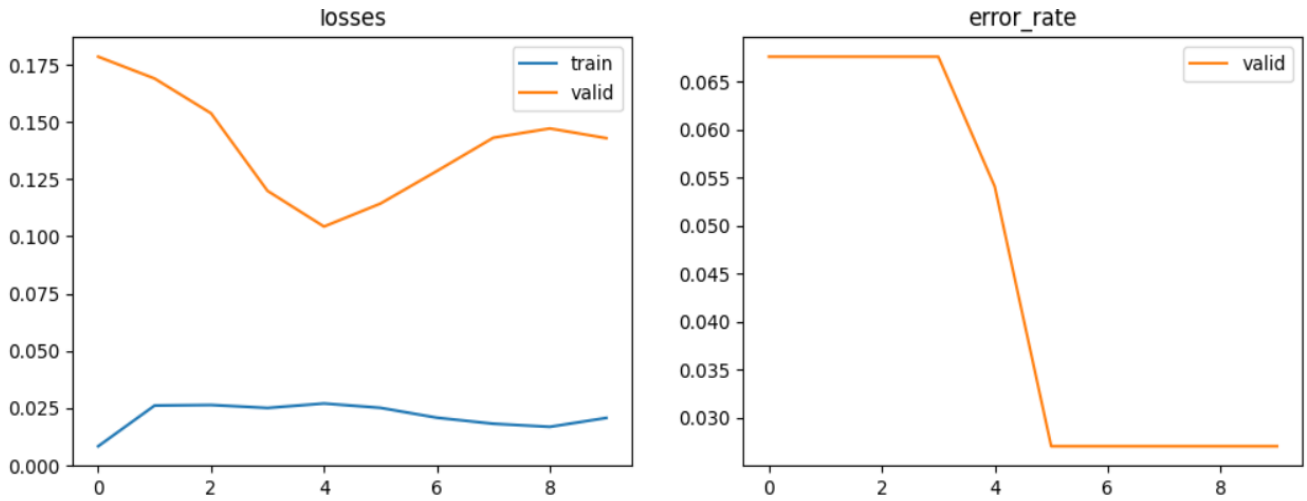

Figure 10. Graphical representation of training loss, validation loss, error rate - DenseNet169

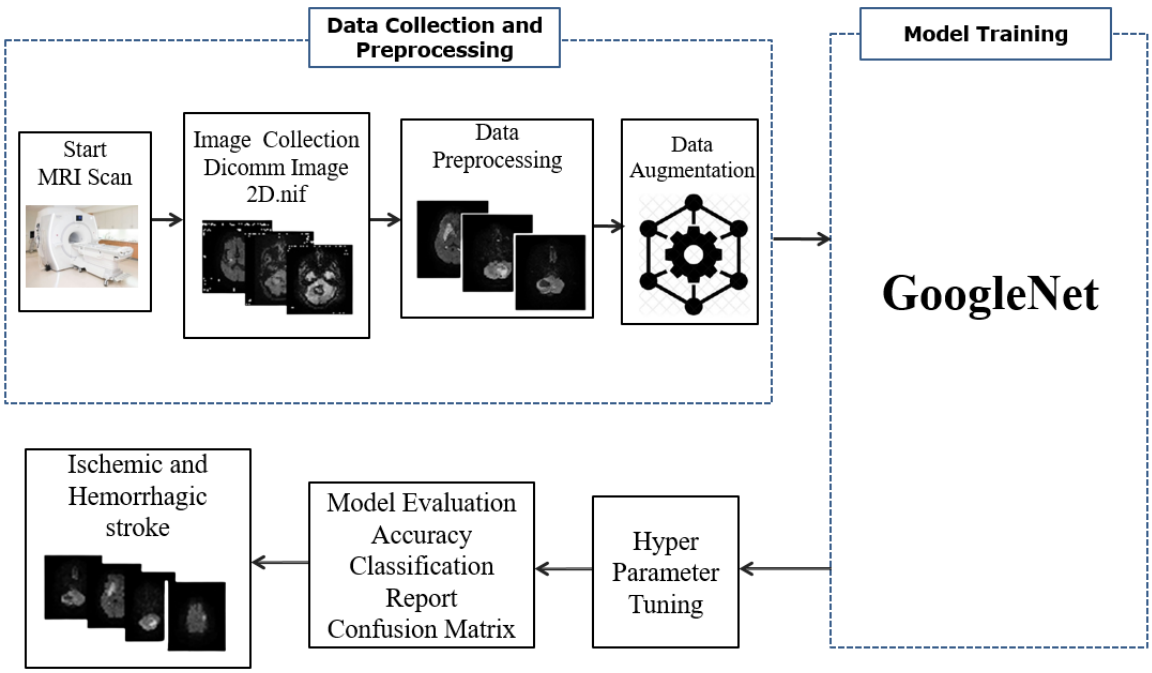

Figure 11. Functional block diagram of GoogleNet

Table 3 displays the duration of the epochs in relation to training, validation loss, and error rate for DenseNet169.

GoogleNet enables the network to select among several sizes of convolutional filters within each block. GoogleNet classifies the stroke such as Figure 11.

Table 3. Table of training epochs, validation loss, error rate - DenseNet169

Epoch	Train_Loss	Val_Loss	Err_Rate	T (ms)
0	0.008398	0.178468	0.067568	00:15
1	0.026188	0.168924	0.067568	00:11
2	0.026426	0.153743	0.067568	00:09
3	0.025125	0.119887	0.067568	00:06
4	0.027084	0.104305	0.054054	00:07
5	0.025176	0.114345	0.027027	00:08
6	0.020868	0.128558	0.027027	00:07
7	0.018236	0.143093	0.027027	00:09
8	0.016894	0.147130	0.027027	00:08
9	0.020773	0.142902	0.027027	00:08

4.3 GoogleNet

Parameters are unfrozen to obtain the learning rate as shown in Figure 12. Out of these, the slide and minimum level attained the same finetuning with baseline model by learning rate finder for the GoogleNet.

Figure 13 displays training loss, and validation loss for unfreeze GoogleNet. Training loss and validation loss vary accordingly based on the performance of GoogleNet Training for unfreeze layers.

Figure 14 displays the training loss, validation loss, and error rate for GoogleNet. As the epoch increases, the loss decreases for both training and validation and the error rate becomes constant after particular epochs.

Table 4 displays the duration of the epochs in relation to training, validation loss, and error rate for GoogleNet.

Table 4. Table for epoch over training loss, validation loss, error rate - GoogleNet

Epoch	Train_Loss	Val_Loss	Err_Rate	T (ms)
0	0.067256	0.309870	0.054054	00:04
1	0.065662	0.468366	0.094595	00:05
2	0.053348	0.631338	0.040541	00:04
3	0.045795	0.754385	0.067568	00:04
4	0.035888	0.099786	0.027027	00:07
5	0.045749	0.062681	0.040541	00:04
6	0.042503	0.213060	0.040541	00:05
7	0.043668	0.164291	0.040541	00:05
8	0.038110	0.099508	0.027027	00:04
9	0.033874	0.087336	0.027027	00:05

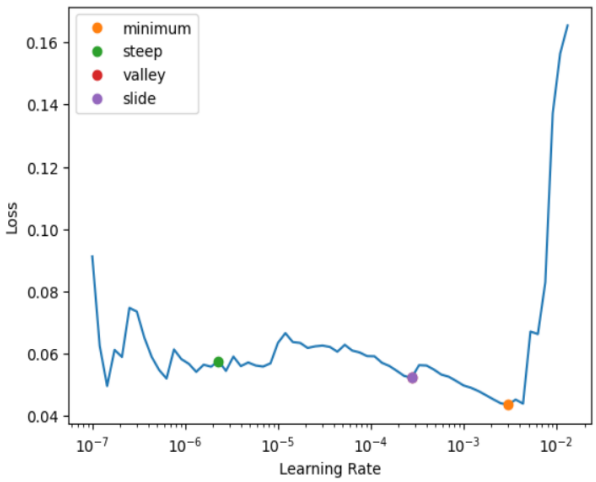

Figure 12. Learning rate finder for GoogleNet

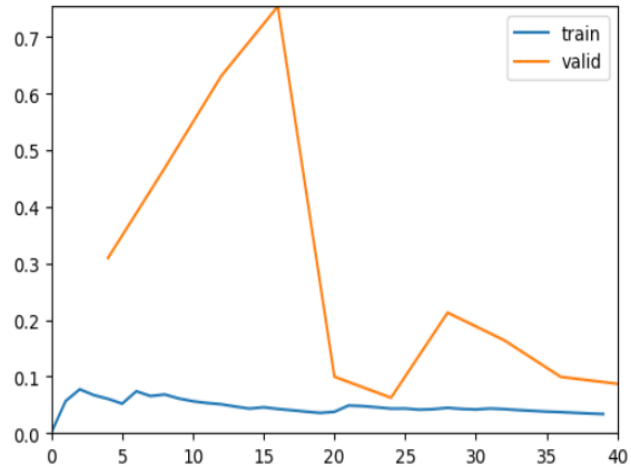

Figure 13. Graphical representation of training loss, validation loss for unfreeze GoogleNet

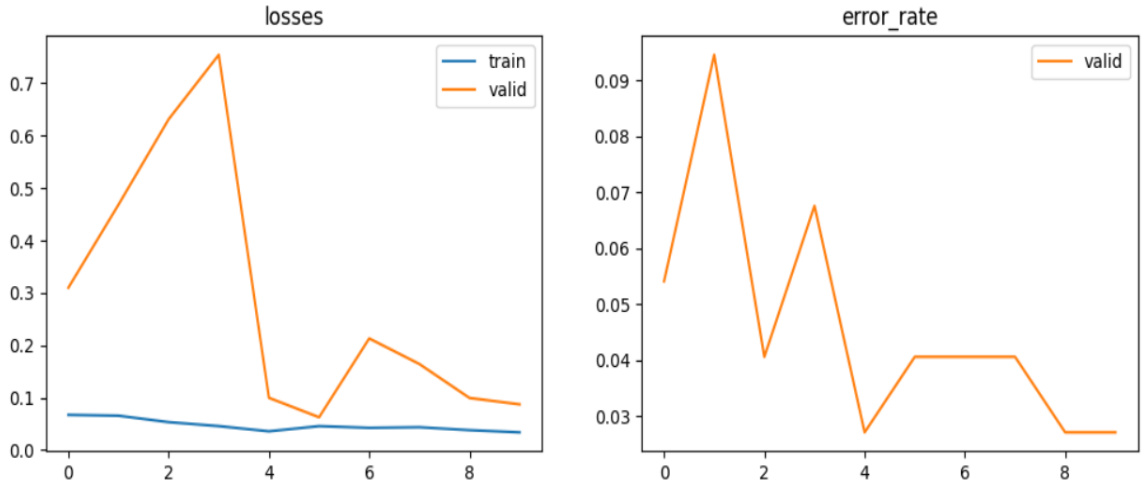

Figure 14. Graphical representation of training loss, validation loss, error rate –GoogleNet

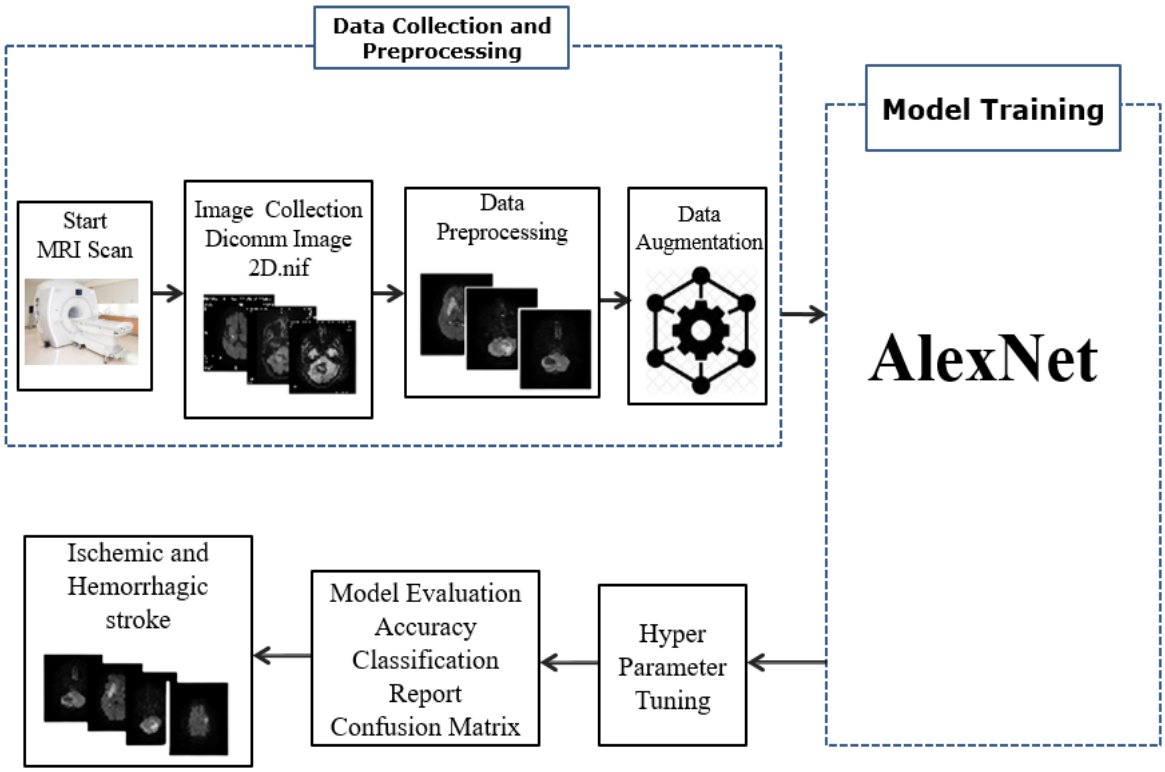

Figure 15. Functional block diagram of AlexNet

4.4 AlexNet

AlexNet has eight layers with learnable parameters. The model comprises five layers, incorporating max pooling, three fully connected layers, and ReLu activation. ReLu activation is applied in each of these layers, except for the output layer. AlexNet classifies the stroke such as Figure 15.

The parameters are unfrozen to obtain the learning rate as shown in Figure 16. Out of these, the minimum level attained the fine tuning with baseline model by the learning rate finder for the AlexNet.

Figure 17 displays training loss and validation loss for unfreeze AlexNet. Training loss, and validation loss vary accordingly based on the performance of AlexNet Training for unfreeze layers.

Figure 18 displays training loss, validation loss, and error rate for AlexNet. As the epoch increases, the loss decreases for both training and validation and the error rate becomes constant Subsequent particular epochs regarding AlexNet.

Table 5 displays the duration of each epoch in relation to training process, validation loss, and error rate for AlexNet model.

Table 5. Table of epochs over training loss, validation loss, error rate - AlexNet

Epoch	Train_Loss	Val_Loss	Err_Rate	T (ms)
0	0.115058	0.607391	0.108108	00:04
1	0.136202	0.943227	0.081081	00:05
2	0.276129	5.404011	0.121622	00:04
3	0.333794	1.628163	0.108108	00:03
4	0.280838	0.321086	0.040541	00:05
5	0.230665	0.059760	0.040541	00:03
6	0.203404	0.133618	0.054054	00:04
7	0.176955	0.121482	0.040541	00:05
8	0.157433	0.120657	0.040541	00:04
9	0.139286	0.144976	0.040541	00:04

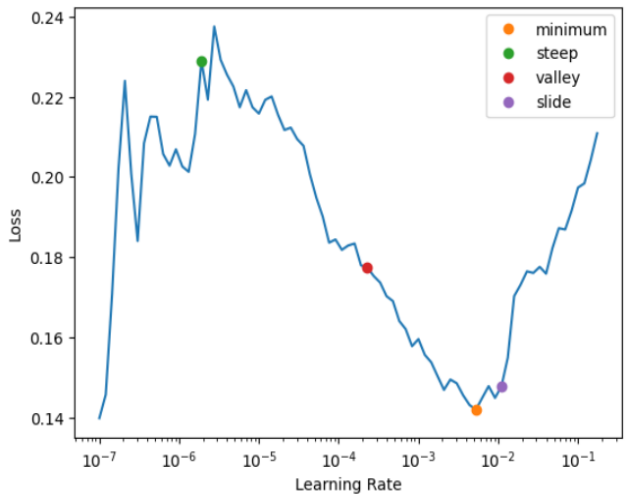

Figure 16. Learning rate finder for AlexNet

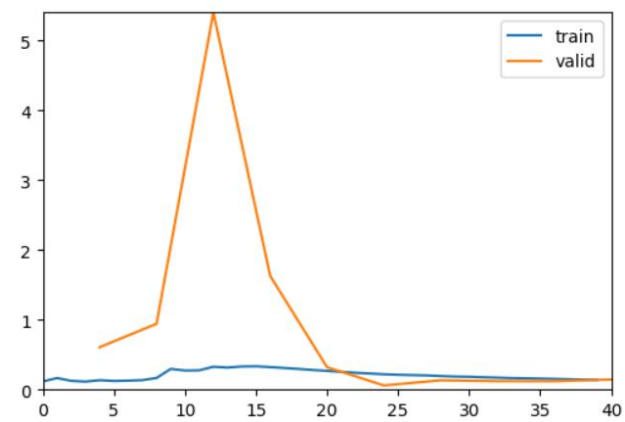

Figure 17. Graphical representation of training loss, validation loss for unfreeze AlexNet

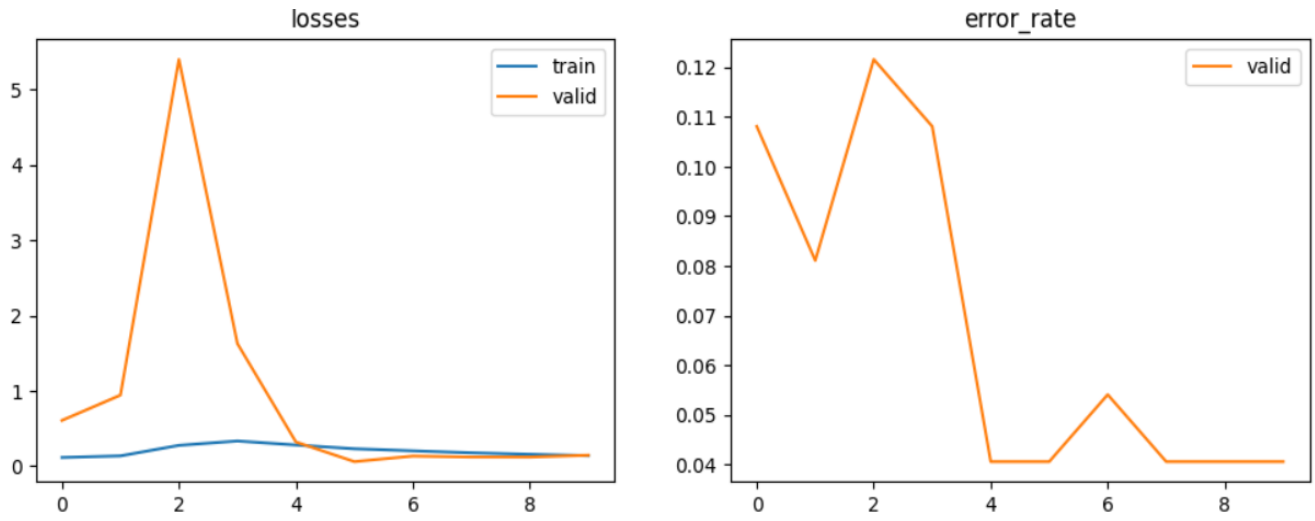

Figure 18. Graphical representation of training loss, validation loss, error rate-AlexNet

As shown in Figure 19, the Ischemic has better precision than Hemorrhagic for all the classifications of CNN Architecture. The Macro Average was treated equally to assess the effectiveness of the classifier for calculating precision regarding stroke. Weighted Average helps to compensate for the imbalances found in the stroke category to classify the Hemorrhagic and Ischemic.

As shown in Figure 20, the Hemorrhagic has better recall than Ischemic for all the classifications of CNN Architecture. The Macro Average was high for DenseNet169 and GoogleNet while ResNet101 and AlexNet were low to classify the recall of stroke. The Weighted Average helps to compensate for the imbalances found in the stroke category to classify the Hemorrhagic and Ischemic.

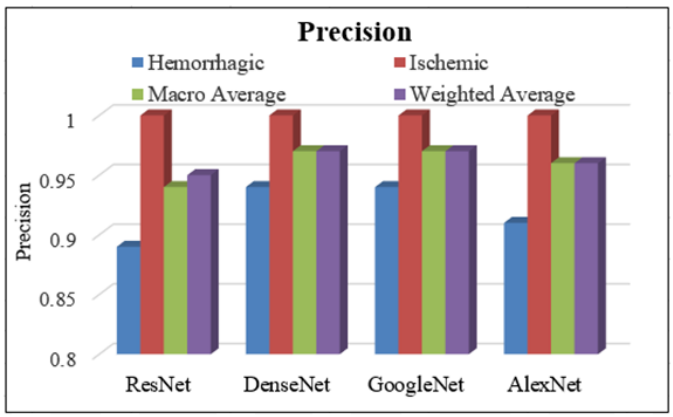

Figure 19. Precision over various CNN architecture

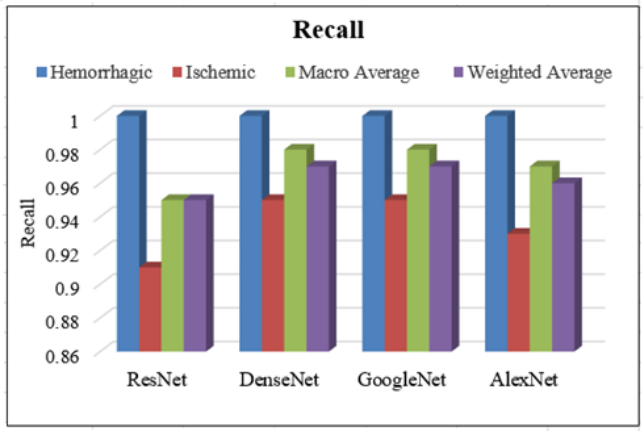

Figure 20. Recall over various CNN architecture

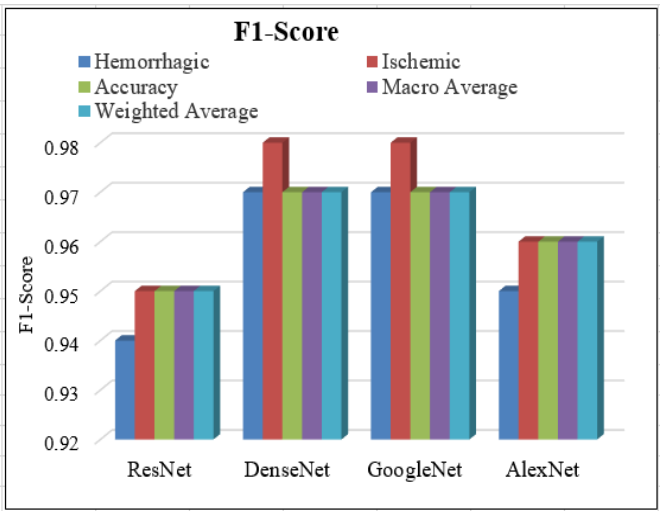

Figure 21. F1 Score over various CNN architecture

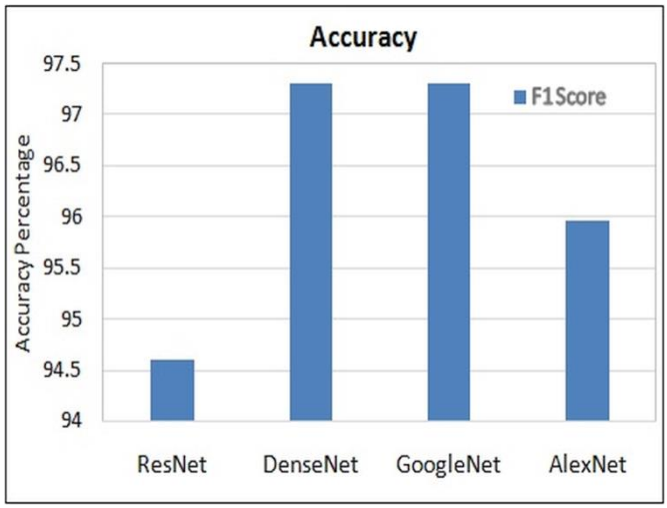

Figure 22. Accuracy for various CNN architecture

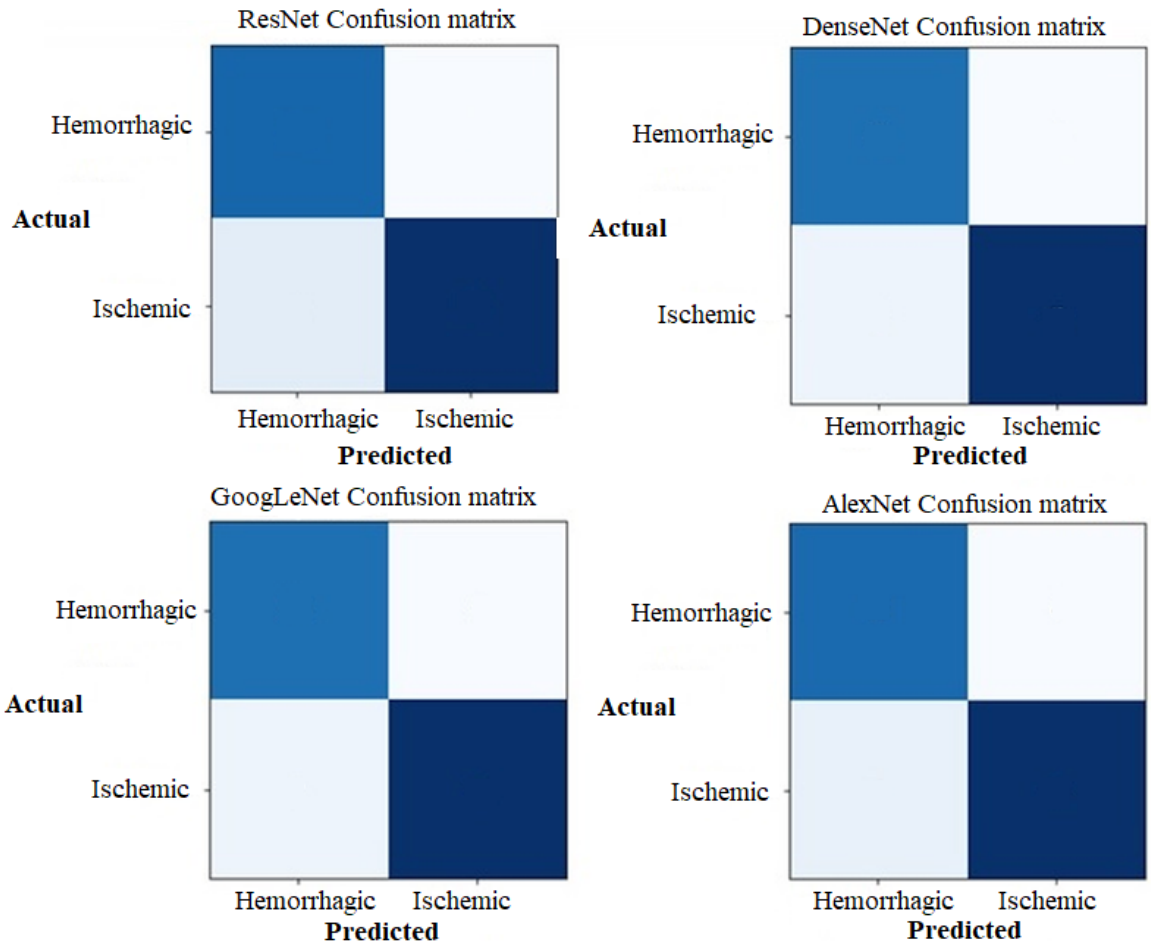

Figure 23. Confusion matrix for various CNN architectures

Table 6. Comparison of existing with proposed work

Paper [Reference]	Accuracy (%)
Li et al. [8]	98 for CT Images
Zhang et al. [7]	92
DenseNet [Proposed]	97.3
AlexNet [Proposed]	97.3
GoogleNet [Proposed]	95.95
ResNet101 [Proposed]	94.59

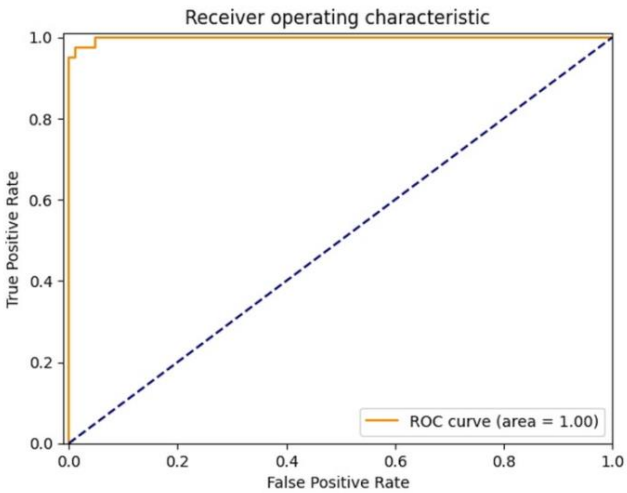

Figure 24. Receiver operating characteristic curve

As shown in Figure 21, the DenseNet169 and GoogleNet F1 score of Ischemic is high when compared to the F1 score of ResNet101 and AlexNet. The CNN Architecture maintains stable F1 score of Hemorrhagic, macro average, and weighted average while variations can be seen for Ischemic.

As shown in Figure 22, DenseNet169 and GoogleNet models have achieved the highest accuracy of 97.3%, while AlexNet has attained 95.95% and ResNet has obtained the accuracy of 94.59%.

The confusion matrix shown in Figure 23 is to categorize the existence of ischaemic and Hemorrhagic MR pictures based on all potential results using a real-time dataset.

GoogleNet and DenseNet169 classifies quiet good number for presence of Ischemic and Hemorrhagic MR images while AlexNet and ResNet101 classifies Ischemic and Hemorrhagic MR images too close to other architectures.

Table 6 shows Comparison of existing with various Net towards accuracy.

Figure 24 shows ROC curve for overall performance of a classification model at various thresholds and ROC area is 0.9984939759036144.

5. CONCLUSIONS

The existing medical imaging system helps to identify the presence of stroke but fails to differentiate and classify the type of stroke they belong. The novelty of the suggested approach addresses the challenges posed by limitations regarding existing by differentiating the stroke type with the help of DWI, GRE, and SWI. CNN Architecture such as

ResNet101, DenseNet169, AlexNet, and GoogleNet has been used to classify the presence of stroke as hemorrhage and ischemic with the support of DWI, GRE, and SWI. The models were trained on real-time dataset of MRI images to achieve high accuracy. The results show that DenseNet169 and GoogleNet has the highest classification accuracy, of 97.3%, while ResNet101 has 94.59%, and AlexNet achieved an accuracy of 95.95%. These models can aid during the initial stages of identification and diagnosis regarding stroke cases, which can lead to faster and more effective treatment, ultimately improving patient well-being. However, Additional investigation is required to verify the efficiency of these models on larger scale and more diverse datasets, ultimately leading to the advancement of more powerful and accurate brain-stroke classification tools.

REFERENCES

[1] Mak, J., Kocanaogullari, D., Huang, X., Kersey, J., Shih, M., Grattan, E.S., Skidmore, E.R., Wittenberg, G.F., Ostadabbas, S., Akcakaya, M. (2022). Detection of stroke-induced visual neglect and target response prediction using augmented reality and electroencephalography. IEEE Transactions on Neural Systems and Rehabilitation Engineering, 30: 1840-1850. https://doi.org/10.1109/TNSRE.2022.3188184

[2] Alanazi, E.M., Abdou, A., Luo, J. (2021). Predicting risk of stroke from lab tests using machine learning algorithms: Development and evaluation of prediction models. JMIR Formative Research, 5(12): e23440. https://doi.org/10.2196/23440

[3] Subbanna, N.K., Rajashekar, D., Cheng, B., Thomalla, G., Fiehler, J., Arbel, T., Forkert, N.D. (2019). Stroke lesion segmentation in FLAIR MRI datasets using customized Markov random fields. Frontiers in Neurology, 10: 541. https://doi.org/10.3389/fneur.2019.00541

[4] Bandi, V., Bhattacharyya, D., Midhunchakkravarthy, D. (2020). Prediction of brain stroke severity using machine learning. Revue d'Intelligence Artificielle, 34(6): 753-761. https://doi.org/10.18280/ria.340609

[5] Guo, L., Khosravi-Farsani, M., Stancombe, A., Bialkowski, K., Abbosh, A. (2021). Adaptive clustering distorted born iterative method for microwave brain tomography with stroke detection and classification. IEEE Transactions on Biomedical Engineering, 69(4): 1512-1523. https://doi.org/10.1109/TBME.2021.3122113

[6] Subudhi, A., Jena, S.S., Sabut, S. (2019). Automated detection of brain stroke in MRI with hybrid fuzzy C-means clustering and random forest classifier. International Journal of Computational Intelligence and Applications, 18(3): 1950018. https://doi.org/10.1142/S1469026819500184

[7] Zhang, Y., Wu, J., Liu, Y., Chen, Y., Wu, E.X., Tang, X. (2020). MI-UNet: multi-inputs UNet incorporating brain parcellation for stroke lesion segmentation from T1-weighted magnetic resonance images. IEEE Journal of Biomedical and Health Informatics, 25(2): 526-535. https://doi.org/10.1109/JBHI.2020.2996783

[8] Li, L., Wei, M., Liu, B. O., Atchaneeyasakul, K., Zhou, F., Pan, Z., Kumar, A.S., Zhang, J.Y., Pu, Y., Liebeskind, D.S., Scalzo, F. (2020). Deep learning for hemorrhagic lesion detection and segmentation on brain CT images. IEEE Journal of Biomedical and Health Informatics, 25(5): 1646-1659. https://doi.org/10.1109/JBHI.2020.3028243

[9] Yu, J., Park, S., Kwon, S.H., Cho, K.H., Lee, H. (2022). AI-based stroke disease prediction system using ECG and PPG bio-signals. IEEE Access, 10: 43623-43638. https://doi.org/10.1109/ACCESS.2022.3169284

[10] Dourado Jr, C.M., Da Silva, S.P.P., da Nobrega, R.V.M., Barros, A.C.D.S., Reboucas Filho, P.P., de Albuquerque, V.H.C. (2019). Deep learning IoT system for online stroke detection in skull computed tomography images. Computer Networks, 152: 25-39. https://doi.org/10.1016/j.comnet.2019.01.019

[11] Tursynova, A., Omarov, B., Tukenova, N., Salgozha, I., Khaaval, O., Ramazanov, R., Ospanov, B. (2023). Deep learning-enabled brain stroke classification on computed tomography images. Computers, Materials & Continua, 75(1): 1431-1446. https://doi.org/10.32604/cmc.2023.034400

[12] Acharya, U.R., Meiburger, K.M., Faust, O., Koh, J.E.W., Oh, S.L., Ciaccio, E.J., Subudhi, A., Jahmunah, V., Sabut, S. (2019). Automatic detection of ischemic stroke using higher order spectra features in brain MRI images. Cognitive Systems Research, 58: 134-142. https://doi.org/10.1016/j.cogsys.2019.05.005

[13] Coli, V.L., Tournier, P.H., Dolean, V., El Kanfoud, I., Pichot, C., Migliaccio, C., Blanc-Féraud, L. (2019). Detection of simulated brain strokes using microwave tomography. IEEE Journal of Electromagnetics, RF and Microwaves in Medicine and Biology, 3(4): 254-260. https://doi.org/10.1109/JERM.2019.2921076

[14] Karthik, R., Menaka, R. (2017). A multi-scale approach for detection of ischemic stroke from brain MR images using discrete curvelet transformation. Measurement, 100: 223-232. https://doi.org/10.1016/j.measurement.2017.01.001

[15] Kodama, T., Kamata, K., Fujiwara, K., Kano, M., Yamakawa, T., Yuki, I., Murayama, Y. (2018). Ischemic stroke detection by analyzing heart rate variability in rat middle cerebral artery occlusion model. IEEE Transactions on Neural Systems and Rehabilitation Engineering, 26(6): 1152-1160. https://doi.org/10.1109/TNSRE.2018.2834554

[16] Zhang, T., Zhang, W., Liu, X., Dai, M., Xuan, Q., Dong, X., Liu, R., Xu, C. (2022). Multifrequency magnetic induction tomography for hemorrhagic stroke detection using an adaptive threshold split Bregman algorithm. IEEE Transactions on Instrumentation and Measurement, 71: 1-13. https://doi.org/10.1109/TIM.2022.3180406

[17] Subudhi, A., Acharya, U.R., Dash, M., Jena, S., Sabut, S. (2018). Automated approach for detection of ischemic stroke using Delaunay Triangulation in brain MRI images. Computers in Biology and Medicine, 103: 116-129. https://doi.org/10.1016/j.compbiomed.2018.10.016

[18] Hu, N., Zhang, T., Wu, Y., Tang, B., Li, M., Song, B., Gong, Q., Wu, M., Gu, S., Lui, S. (2022). Detecting brain lesions in suspected acute ischemic stroke with CT-based synthetic MRI using generative adversarial networks. Annals of Translational Medicine, 10(2): 1-16. https://doi.org/10.21037/atm-21-4056

[19] Kuang, H., Menon, B.K., Qiu, W. (2019). Segmenting hemorrhagic and ischemic infarct simultaneously from

follow-up non-contrast CT images in patients with acute ischemic stroke. IEEE Access, 7: 39842-39851. https://doi.org/10.1109/ACCESS.2019.2906605

[20] Yu, Y., Guo, D., Lou, M., Liebeskind, D., Scalzo, F. (2017). Prediction of hemorrhagic transformation severity in acute stroke from source perfusion MRI. IEEE Transactions on Biomedical Engineering, 65(9): 2058-2065. https://doi.org/10.1109/TBME.2017.2783241

[21] Rodriguez-Duarte, D.O., Origlia, C., Vasquez, J.A.T., Scapaticci, R., Crocco, L., Vipiana, F. (2022). Experimental assessment of real-time brain stroke monitoring via a microwave imaging scanner. IEEE Open Journal of Antennas and Propagation, 3: 824-835. https://doi.org/10.1109/OJAP.2022.3192884

[22] Wang, X., Yi, J., Li, Y. (2023). Cerebral stroke classification based on fusion model of 3D EmbedConvNext and 3D Bi-LSTM network. International Journal of Imaging Systems and Technology, 33(6): 1944-1956. https://doi.org/10.1002/ima.22928

[23] Kaya, B., Önal, M. (2023). A CNN transfer learning-based approach for segmentation and classification of brain stroke from noncontrast CT images. International Journal of Imaging Systems and Technology, 33(4): 1335-1352. https://doi.org/10.1002/ima.22864

[24] Sri Sabarimani, K., Arthi, R. (2021). A brief review on brain tumour detection and classifications. Bio-inspired Neurocomputing, 61-72. https://doi.org/10.1007/978-981-15-5495-7_4